A Novel Gene Required for Male Fertility and Functional CATSPER Channel Formation in Spermatozoa

Published in final edited form as:
Nat Commun. 2011 January 11; 2: 153. doi:10.1038/ncomms1153.

A Novel Gene Required for Male Fertility and Functional CATSPER Channel Formation in Spermatozoa

Jean-Ju Chung, **Betsy Navarro**, **Grigory Krapivinsky**, **Luba Krapivinsky**, and **David E. Clapham***
Howard Hughes Medical Institute, Manton Center for Orphan Disease, Children's Hospital Boston, and the Department of Neurobiology, Harvard Medical School, Boston, Massachusetts 02115

Summary

Calcium signaling is critical for successful fertilization. In spermatozoa, capacitation, hyperactivation of motility, and the acrosome reaction are all mediated by increases in intracellular Ca^{2+}. *Cat*ion channels of *sper*m proteins (CATSPERS1-4) form an alkalinization-activated Ca^{2+}-selective channel required for the hyperactivated motility of spermatozoa and male fertility. Each of the *CatSper1-4* genes encodes a subunit of a tetramer surrounding a Ca^{2+}-selective pore, in analogy with other six-transmembrane ion channel α subunits. In addition to the pore-forming proteins, the sperm Ca^{2+} channel contains auxiliary subunits, CATSPERβ and CATSPERγ. Here, we identify the *Tmem146* gene product as a novel subunit, CATSPERδ, required for CATSPER channel function. We find that mice lacking the sperm tail-specific CATSPERδ are infertile and their spermatozoa lack both Ca^{2+} current and hyperactivated motility. We show that CATSPERδ is an essential element of the CATSPER channel complex and propose that CATSPERδ is required for proper CATSPER channel assembly and/or transport.

Direct recordings of mammalian spermatozoa combined with targeted genetic disruption enabled the precise identification of the sperm ion channel currents that bring calcium into the cell[1]. All mammals and some invertebrate species, contain the genes encoding the alkalinization-activated Ca^{2+}-selective ion channels, *Cat*ion channel of *sper*m (*CatSpers1-4*). Genetic deletion of any of the four *CatSper* genes in mice results in loss of hyperactivated motility and male infertility[2,3,4,5,6,7]. Biochemical studies show that CATSPERS form a heteromeric complex, likely with each of the CATSPERS1-4 subunits surrounding a central Ca^{2+} selective pore, in analogy with other six-transmembrane (6TM)

*Correspondence to: David E. Clapham (dclapham@enders.tch.harvard.edu).

Author Contributions
J-J.C., B.N., G.K. and D.E.C designed and interpreted the experiments. J-J.C. analyzed proteomic data, designed and generated knockout construct, bred the mice and performed phenotype characterization including sperm flagellar waveform analysis. J-J.C. also performed molecular cloning, *in situ* hybridization, RT-PCR, immunostaining, confocal imaging, immunoprecipitation and immunoblotting. B.N. performed electrophysiological recordings of sperm. G.K. and L.K. performed the proteomic purification of CATSPER1 complex. J-J.C. assembled figures and J.J.C and D.E.C wrote the manuscript.

Competing Financial Interest Statement
The authors declare no competing financial interest.

spanning ion channel α subunits[8]. Mutations in *CatSper1* and *CatSper2* are associated with male infertility in humans[9,10,11]. In addition to the pore-forming proteins, the sperm Ca^{2+} channel contains the auxiliary subunits, CATSPERβ and CATSPERγ[12,13].

High amplitude and highly curved movements of the tail characterize hyperactivated motility, which is acquired during capacitation. Hyperactivation serves to generate more force to escape impediments and penetrate barriers such as the *zona pellucida* (ZP)[6,14]. High pH, cyclic nucleotides, *zona pellucida* glycoproteins, and bovine serum albumin all can induce CATSPER -dependent Ca^{2+} influx[1,6,15,16]. Despite extensive characterization of the functional importance of mutant mice of the CATSPER pore-forming α subunits in male infertility, the difficulty of expressing functional CATSPER channels in heterologous systems, singly or in combination, has limited our understanding of the precise mechanism of CATSPER regulation. Studies suggest that the CATSPER complex includes CATSPERS1-4, CATSPERβ, CATSPERγ, and that the complex associates with the chaperone HSPA2 (previously known as HSP70-2)[5,12,13]. CATSPERβ and CATSPERγ express normally in the testis but not in spermatozoa of *CatSper1-null* mice[12,13], suggesting that only correctly assembled CATSPER channel with all subunits traffic to the flagellar membrane of spermatozoa. Attempts to express functional CATSPER channels in heterologous systems, including *Xenopus* oocytes with all known 6 CATSPERS co-expressed with HSPA2, have not been successful. Our working hypothesis is that this failure of heterologous expression is due to the lack of sperm-specific intraflagellar transport machinery and adaptor proteins in these systems. Alternatively, there may be unidentified channel subunits required for proper assembly. To further characterize the CATSPER complex, we performed proteomic analyses with tandem affinity purification followed by mass spectrometry. As a result of these attempts, we identified a novel auxiliary subunit, CATSPERδ (TMEM146), and verified the previously reported CATSPERβ[14] and CATSPERγ[15] auxiliary subunits in the CATSPER complex. *CatSperβ, γ,* and *δ* mRNAs appear in unison 6d before *CatSperα* subunit mRNAs in young mice. In mice lacking *CatSperδ*, CATSPERβ and CATSPERγ form a stable complex while CATSPER1 is substantially reduced, suggesting that CATSPERδ is important for the stability of CATSPER1 and CATSPER complex formation. Most importantly, *CatSperδ-null* mice spermatozoa lack $I_{CatSper}$, fail to hyperactivate, and are infertile, demonstrating that CATSPERδ is required for proper CATSPER complex formation and ion channel function.

Here we demonstrate that the murine *Tmem146* gene encodes CATSPERδ, a critical subunit of the CATSPER ion channel complex. Targeted disruption of *CatSperδ* abrogated CatSper current, hyperactivated motility and male fertility. We show CATSPERδ association with CATSPER1 is essential for the stability of the CATSPER1 protein before intraflagellar transport and/or incorporation of the CATSPER channel complex into the flagellar membrane.

Results

Proteomic identification of CATSPER complex proteins

We purified a CATSPER1-containing protein complex from solubilized mouse testes microsomes. To perform purification, we took advantage of the abundance of histidines in

the amino terminus of CATSPER1 (51/250 amino acids in the amino terminus) by using metal chelation chromatography and then further enriched the CATSPER1-containing molecular complex by immunoaffinity chromatography with anti-CATSPER1-specific antibody. Proteins of the purified anti-CATSPER1 complex were resolved on SDS-PAGE (Fig. 1a, α-CATSPER1). Numbered protein bands were excised from the gel, digested with trypsin, and identified using mass spectrometry. Among the identified proteins, confirmed CATSPER1 interactors are listed in Fig. 1a. The complete list of proteins that copurified with CATSPER1 is provided in Table 1. The previously reported CATSPERS1-4 and its auxiliary subunits, CATSPERβ, CATSPERγ, and HSPA2 were identified in the purified CATSPER1 molecular complex.

A number of purified molecules were eliminated from consideration as CATSPER complex proteins. Among these were two members of solute carrier family, SLC39A6 and SLC39A7. Since these proteins were not testis-specific and did not interact specifically with CATSPER 1 (Fig. 1, b and c), they were likely enriched during purification simply due to the abundance of their histidine residues. Two previously unidentified candidate proteins were detected from band 12; the unannotated hypothetical protein, LOC75721 (NP_898936, Accession No. 34147101) and the uncharacterized protein annotated as TMEM146 (Accession No. 261245039). Hypothetical protein LOC75721 has no mammalian orthologs and has no transmembrane domains. Despite its expression in the testis, it was not found in the CATSPER1 immune complex nor was it expressed in spermatozoa (Fig. 1d). In contrast, a polyclonal antibody to the very C-terminal region of TMEME146 (RRVKDQNRGKVRVAQKHPET) specifically recognized the ~85 kDa TMEM146 protein in CATSPER1 immunoprecipitates, confirming association of the two proteins (Fig. 1e). Analysis of amino acid sequences predicted that TMEM146 has one putative transmembrane domain but no homology to any other proteins of known function. We refer to the *Tmem146* gene product as CATSPERδ.

Cloning of *CatSperδ*

Among the many tissues examined, *CatSperδ* mRNA was detected only in testis (Fig. 2a), as previously found for *CatSpers1-4*, *CatSperβ*, and *CatSperγ*[4,5,6,12,13,17]. The initial mouse *Tmem146* cDNA sequences were identified from database searches using novel peptide sequences from mass spectrometry. These predicted polypeptides (AK077082: 448 amino acids and XM_001052081: 486 amino acids) were much smaller than that predicted from the apparent molecular weight of the band observed in Fig. 1e or that predicted for human TMEM146 (798 a.a, see Supplementary Fig. S1). Moreover, the two cDNAs shared a common C-terminus homologous to the C-terminus of human TMEM146. Therefore, 5′-RACE was used to extend the open reading frame and RT-PCR was performed to further characterize the two potential splice variants identified. Two products differing by 118 bp were amplified (Fig. 2b and Supplementary Fig. S1). The 118 bp insertion in the 5′-UTR of the small transcript creates a new start site in the open reading frame. The longer splice variant encodes a protein similar in size to other mammalian *Tmem146* orthologues (*Tmem146-l*, Supplementary Fig. S1). Whole open reading frames (ORFs) of the mouse *Tmem146* gene were identified by PCR of mouse testis first strand cDNAs (Fig. 2c). The PCR product between 2 and 2.5 kb was cloned and sequenced, yielding *Tmem146-l* and

Tmem146-s. The nucleotide sequences of *Tmem146-l* (accession no. HQ441159) and *Tmem146-s* (accession no. HQ441160) were deposited into GenBank. We conclude that the mouse *Tmem146* gene located on mouse chromosome 17 consists of 22 exons and expresses at least two potential splice variants that can encode protein isoforms of 661 (TMEM146-s) and 805 (TMEM146-l) amino acids in length (Fig. 2, d and e).

Restricted expression of *CatSperδ* mRNAs in testis

To determine the expression pattern of *CatSperδ* mRNA within testis, we performed *in situ* hybridization. Two RNA probes were generated by nested PCR amplification of different regions of *Tmem146-s* cDNA by incorporation of T7 and SP6 RNA polymerase promoters[18]. A single RNA band was observed from each *in vitro* transcription. Probe 1, complementary to exons 14–22, was used to recognize both *Tmem146-s* and *Tmem146-l* transcripts (Fig. 2d) and detected *CatSperδ* in spermatocytes and spermatids in different stages of spermatogenesis (Fig. 2f). This expression pattern is similar to that reported for *CatSperβ* and *γ*[12,13]. Probe 2 was designed to span the splice junction of exon 4 and 6 of *Tmem146-s* mRNA, the region unique to the *Tmem146-s* sequence (Fig. 2d). Probe 2 revealed more restricted expression at an early stage of spermatogenesis (Fig. 2f), suggesting that *Tmem146-s* mRNA expression occurs prior to *Tmem146-l*. Interstitial cells were not labeled by *in situ* hybridization by either probe. Using real time PCR, *Tmem146-s* mRNA was first detected at 17 day while *Tmem146-l* appeared at 20 day of testis development (Fig. 2g), consistent with the *in situ* hybridization experiments.

CATSPERδ, a single transmembrane-spanning protein of the sperm tail

Mouse CATSPERδ encoded by *Tmem146-l* is predicted to be 805 amino acids in length with a predicted molecular weight of 91 kDa (pI 6.68; Fig. 3a). Hydrophilicity plots of mouse and human CATSPERδ suggest that mouse CATSPERδ has one signal peptide, a large extracellular domain of 699 amino acids followed by a transmembrane-spanning domain and ending in an intracellular tail of 60 amino acids (Fig. 3b). The predicted transmembrane topology is similar to CATSPERγ. The amino acid sequence of mouse CATSPERδ is not similar to any other protein with known function. CATSPER α, β and γ subunits have the same evolutionary pattern; their orthologs are present in the genomes of mammals, as well as sea squirts (*Ciona intestinalis)*, and sea urchins (*Strongylocentrotus purpuratus*)[19]. In contrast, *CatSperδ* orthologues were found only in mammals and a reptile (*Anolis carolinensis*, a green lizard), implying that *CatSperδ* imparts a species-specific function. Like many gamete-specific proteins[19], CATSPERδ shows signs of rapid evolutionary change since sequence identity between human and mouse CATSPERδ is relatively low (51%; Supplementary Fig. S1).

CATSPERδ is strictly localized to the principal piece of spermatozoa (Fig. 3c), like all other CATSPER ion channel complex proteins[5,6,7,12,13]. CATSPERδ was detected in *wt* and *CatSper1-null* testis (Fig. 3d), but not in mature *CatSper1-null* spermatozoa (Fig. 3e). This result is concordant with CATSPERβ and CATSPERγ expression in mice lacking *CatSper1*[12,13] (see also Fig. 3, d and f). Thus, the expression of auxiliary subunits of CATSPER channel in sperm cells depends on the presence of CATSPER1 and presumably other pore-forming α subunits, suggesting that complete and proper assembly of CATSPER

channel complex is a prerequisite to intraflagellar trafficking, insertion of the complex into the flagellar membrane, or both.

Targeted disruption of *CatSperδ*

Since reconstitution of functional CATSPER channels has not succeeded in any heterologous system, genetic manipulation remains the primary tool to study the function of CATSPER subunits. Interestingly, mouse *CatSperβ* and *CatSperγ* genes were duplicated at some point in evolution. *CatSperβ* and its partial duplicate are separated by ~ 37 kb apart on chromosome 12, while copies of *CatSperγ* are separated by 480 kb on chromosome 7. These duplications complicate genetic disruption of *CatSperβ* and *CatSperγ*. In contrast, only a single copy of *CatSperδ* is found in the mouse genome. Thus we generated a *CatSperδ-null* mouse line lacking CATSPERδ using the recombineering technique[20]. Following homologous recombination, exon 9 was excised by *Cre*-recombinase in embryonic stem (ES) cells (Fig. 4a). Deletion of exon 9 resulted in a frame-shift and generated multiple downstream stop codons, thereby inactivating both *Tmem146-s* and *Tmem146-l* transcripts (Fig. 4a and Supplementary Fig. S1). PCR screening of flanking regions of the targeting construct revealed clones with successful homologous recombination (Fig. 4b). Deletion of exon 9 was confirmed in the smaller PCR product of the genomic sequence in the *Cre*-catalyzed ES clone (Fig. 4c, *97-Cre*). Absence of exon 9 in the *CatSperδ* transcript of homozygous null mice was confirmed by RT-PCR of testis mRNA (Fig. 4d). No CATSPERδ was detected in *CatSperδ–null* spermatozoa as determined by immunocytochemistry (Fig. 4e) and immunoblotting (Fig. 4f).

CatSperδ is required for male fertility

CatSperδ-null mutant mice are indistinguishable from their *wt* or heterozygous *(het)* littermates in appearance, gross behavior, and survival. In addition, no morphological differences were observed by histological examination of testis and epididymis (Fig. 5a). *CatSperδ-null* female mice exhibited normal mating behavior and gave birth to litters comparable to those of *wt* females when mated with *wt* or *het* males. However, when *CatSperδ-null* male mice were mated with *wt* or *het* females (4 pairs for > 3 months), no litters was produced, indicating that *CatSperδ-null* male mice are completely infertile. In contrast, 18 litters were produced as offspring of 5 pairs of heterozygous males and females, yielding 128 pups (31 *wt*, 67 *het*, 30 *null*) in a Mendelian ratio with an average of 7.1 pups per litter during the same period (Fig. 5b), and similar to 7.8 pups/litter for *wt* mice[5]. The sperm count from *CatSperδ* homozygous *null* mice was slightly lower than that of paired littermate heterozygous mice at 2–3 months of age, but was not significantly different at 7–8 months of age (Fig. 5c). *Tmem146/CatSperδ* is reportedly reduced in tetrazoospermic patients (GDS2697/237020_at/Tmem146 in GEO profiles)[21], but more studies are warranted to examine the roles of the two isoforms during early spermatogenesis.

CatSperδ-null spermatozoa fail to hyperactivate and lack $I_{CatSper}$

Bicarbonate increases mammalian spermatozoa motility by stimulating soluble adenylyl cyclase (ADCY10)[22,23]. We tested bicarbonate-evoked activation of motility in *CatSperδ-null* sperm and found that activated motility was preserved in both *CatSperδ-null* (9.5 ± 0.4

Hz) and *CatSperδ-het* (5.7 ± 0.2 Hz) mouse spermatozoa compared to sperm cells under non-capacitating conditions (Fig. 5d; time 0 vs. 10 min, $P = 10^{-11}$ for *CatSperδ-null; P* = 10^{-5} for *CatSperδ-het* sperm, ***; compare Supplementary Movies 1, 2, 3 and 4). This result is consistent with prior reports showing that CATSPER1 and 2 are not required for the initial activation of flagellar beating[2,3] induced by cAMP after bicarbonate-activation of soluble adenylyl cyclase (ADCY10). In contrast, *CatSperδ-null* sperm fail to develop hyperactivated motility as was also observed in *CatSpers1-4* mutant sperm cells (compare Supplementary Movies 5 and 6). After 90 min under capacitating conditions, beat frequency significantly decreased in *CatSperδ-het* spermatozoa (4.6 ± 0.2 Hz) when compared to that of activated sperm (5.7 ± 0.2 Hz; Fig. 5d, 10*vs*. 90 min, **, $P = 0.0012$). Flagellar amplitudes of *CatSperδ-het* spermatozoa (and *wt*, see ref. 3) were substantially larger than that of capacitated *CatSperδ-null* spermatozoa (Fig. 5e). In contrast, capacitating conditions did not substantially change the flagellar amplitude of *CatSperδ-null* spermatozoa (compare Supplementary Movies 3, 4, 5, and 6). Aligned flagella waveform traces of representative sperm reveal the lower frequency of movement in *het* spermatozoa (one averaged full beat cycle = 225 ms compared to 175 ms in activated sperm cells). In comparison, *CatSperδ-null* sperm complete one cycle in 108 ms under the same capacitating conditions (Fig. 5e, Supplementary Fig. S2). These changes are consistent with previous reports in *CatSper1-null* mice[3].

Another well-established feature of hyperactivated spermatozoa is an increase in the angle between head/midpiece and the principal piece known as the bend angle[2,5]. In *CatSperδ-null* mice, the maximum bend angle (α) of the principal bend in the midpiece was 56 ± 3° relative to 0° (straight), significantly smaller than the 117 ± 10° bend angle recorded in *het* spermatozoa under capacitating conditions (Fig. 5f, unpaired two-tailed *t*-test, $P = 0.0018$).

$I_{CatSper}$ is a sperm-specific, Ca^{2+}- selective, pH-sensitive ion current mediated by CATSPER proteins[1]. $I_{CatSper}$ is small and difficult to record in normal 2 mM Ca^{2+} bath solution. As is typical for Ca^{2+}- selective channels, this is remedied by recording in divalent-free (DVF) solution where $I_{CatSper}$ is carried by Na^+ ions[1]. In *CatSperδ-het* spermatozoa, $I_{CatSper}$ mediates a large Na^+ inward current (−950 ± 190 pA at −100 mV; Fig. 6a), indistinguishable from previously recorded *wt* spermatozoa[1]. In sperm from *CatSperδ-null* mice, monovalent CATSPER current was not detected (<−9 ± 8 pA at −100 mV; Fig. 6b), consistent with the absence of current in mice lacking *CatSpers 1, 2, 3,* or *4*[1,5]. In addition, expression of *CatSperδ* with *CatSper1, 2, 3, 4, β,* and *γ*, as well as *Hspa2* failed to yield detectable ion currents in *Xenopus* oocytes, suggesting that the CATSPER complex is still incomplete, or that specific flagellar proteins are required for proper membrane insertion of a CATSPER complex.

I_{KSper} is a pH-sensitive K^+ current in sperm[8] mediated by the mSLO3[24,25] and is responsible for hyperpolarization of spermatozoa during capacitation[26]. By hyperpolarizing the spermatozoan membrane potential to −50 mV[8,26], it increases the driving force for Ca^{2+} entry via the CATSPER channel. In *CatSperδ-null* spermatozoa, I_{KSper} did not differ substantially from heterozygous spermatozoa (Fig. 6).

Inactivation of *CatSperδ* decreases the stability of CATSPER1

CATSPERS3, 4, β and γ are expressed in testis, despite their absence in the principal piece of sperm cells in *CatSper1-null* mice[5,13,20]. In testis they are present in the endoplasmic reticulum and Golgi apparatus, as is typical for proteins during assembly. Similarly, CATSPERδ levels are indistinguishable from *wt* in the testes of mice lacking *CatSper1*. However, CATSPERδ does associate with CATSPERβ in the testis of these mutant mice (Fig. 3d). We next examined the expression and association of other CATSPERS in the testis and spermatozoa of *CatSperδ-null* mice. Strikingly, ablation of *CatSperδ* dramatically reduced CATSPER1 levels in the testis (Fig. 7a input). Real-time qRT-PCR results indicate that *CatSper1*, *CatSperβ*, and *CatSperγ* mRNA expression in testes were not substantially different in *CatSperδ-null* compared to *CatSperδ-het* mice (Supplementary Fig. S3), suggesting that transcriptional regulation is not responsible for the CATSPER1 reduction observed in *CatSperδ-null* mice and that CATSPER1 is subject to degradation if not assembled properly with CATSPERδ. Collectively, these data indicate that progression of the CATSPER complex from the Golgi/ER to the flagellar membrane requires proper assembly of the complex.

mRNA expression of *CatSpers1-4* is reportedly developmentally regulated during mouse sexual maturation. *CatSper2* mRNA is first detected at postnatal day 18, and the mRNAs of *CatSper3*, *4*, and *CatSper1* follow at postnatal day 21, 21 and 21–25, respectively[27,28]. To obtain more insight into the potential roles of CATSPERδ in the assembly, stability, or transport of the CATSPER complex, temporal mRNA expression of the *β, γ* and *δ CatSper* auxiliary subunits was compared to *CatSper1* expression by real-time PCR during postnatal testis development. mRNA of auxiliary subunits appeared around postnatal day 17, earlier than the initiation of *CatSper1* mRNA expression (postnatal day 23, consistent with ref 27 and 28; Supplementary Fig. S3). These data suggest that CATSPERδ, CATSPERβ, and CATSPERγ are likely to be synthesized before and during CATSPER1 expression. The dramatic reduction of CATSPER1 (Fig. 7a), the preservation of interaction between other auxiliary subunits in testes of *CatSperδ-null* mice (Fig. 7b), and the absence of all CATSPER proteins in spermatozoa of *CatSperδ-null* mice (Fig. 4f and Fig. 7c) suggests that CATSPERδ assembly with CATSPER1 is required to prevent CATSPER1 degradation. CATSPERδ may have additional functions in transport and/or membrane insertion of the CATSPER channel complex.

Discussion

CATSPER channels are unique, sperm-specific, Ca^{2+} -selective ion channels. As we have shown in previous papers and in the present work, the CATSPER channel is much more complex in its protein composition than all other ion channels to date. First, four independent genes encode each α subunit of the tetrameric Ca^{2+} -selective pore, compared to the one α subunit gene encoding the 4 × 6TM repeat structure of Ca_V channels, or the one gene that encodes the tetrameric Ca^{2+} -selective channels such as Orai1, TRPV5, or TRPV6. The common theme amongst all these channels is that the α subunits position the pore lining residues into the center of the protein, shielding the transfer of charge across the lipid bilayers. Each CATSPER α subunit contains a pair of negatively charged aspartic acid

residues that, by inference from work on other Ca^{2+} channels, come together to bind Ca^{2+} within the pore and confer its Ca^{2+} ion selectivity. A second unusual feature of CATSPER channels is that each voltage-sensing domain (S1–S4) differs from the others. In other voltage-sensing channels, the S1–S4 domain contains positively charged (usually arginine) amino acids every third residue in the 4th transmembrane spanning segment (S4). In the CATSPER complex, CATSPER1 generally follows this convention, while CATSPERS 4, 2, and 3 have increasingly fewer charged residues. The end result is that CATSPER is only weakly voltage-sensitive. Perhaps at an early stage of evolution, this voltage gating property was important, but has been progressively lost. A third unusual feature is CATSPER1's histidine-rich amino terminus. Since heterologous expression of the CATSPER complex is not currently possible to conduct mutagenesis studies, we can only surmise that these histidines may be important for CATSPER channel proton sensitivity or Zn^{2+} binding.

Like CATSPER, Ca_V channels have auxiliary subunits, defined as protein subunits that do not directly participate in pore formation. Ca_V1 and Ca_V2 α1 subunit commonly associate with proteins named α2δ and β, but these have no homology to the CATSPER β, γ, and δ subunits. The topology of Ca_v α2δ is similar to CATSPERs γ and δ in that all three have a single transmembrane spanning domain and a large extracellular amino terminal loop. Ca_v channel auxiliary subunits are not required for expression but rather appear to modulate expression levels and channel kinetics[29,30]. In contrast, as we have shown here, CATSPERδ, is required for CATSPER channel α subunit expression and function. In spermatozoa, the constraints on channel trafficking are more stringent than for other ion channels in non-sperm cells. For the CATSPER complex, seven distinct gene products must be assembled and targeted specifically to the principal piece of the sperm tail. The tail, being a flagellar/ciliary structure, employs an intraflagellar transport system for protein targeting[31]. Thus, one or more of the CATSPER auxiliary subunits may be important for adapting to flagellar transport motors or the complex's insertion into the membrane. Another possibility is that one or more of the auxiliary subunits are important for assembly in the ER or Golgi apparatus. Although mRNA levels do not accurately report protein levels, all *CatSper* auxiliary subunit mRNAs appear well before *CatSper*α subunit mRNAs during postnatal development. In addition, none of the *CatSper1, 3,* or *4 null* mutants affected expression levels of auxiliary subunits (Fig. 3f). Thus, one possibility is that the auxiliary subunits must appear prior to CATSPERα subunits to enable their proper assembly. In support of this notion, *CatSperδ* ablation resulted in much reduced detected CATSPER1 α subunit, suggesting that one function of the auxiliary subunits may be to prevent CATSPERs from proteosomal degradation before or during transport. As an example, the voltage-sensing domain of CATSPER1 may require a chaperone during assembly as proposed for ancillary subunits of Kv4 channels[32].

The fact that all the CATSPER auxiliary subunits have large extracellular domains raises the question of whether they bind factors that might initiate or alter CATSPER channel gating. It will be important to understand the structure of these domains and determine whether they bind potential gating agents, such as reproductive hormones (*e.g.* progesterone), chemoattractants, or surface recognition molecules.

Our study identifies CATSPERδ, encoded by the *Tmem146* gene, as being required for male fertility via its crucial role in the CATSPER channel complex. The phenotypes for mice in which any of the *CatSper1-4* or *CatSperδ* genes are ablated are practically identical, with each displaying complete loss of $I_{CatSper}$ and consequent failure of hyperactivated motility, gradual loss of progressive motility over time, and complete male infertility. One minor difference appears to be a slight decrease in *CatSperδ-null* sperm counts in young animals, but a role for *CatSperδ* isoforms in spermatogenesis will require much more detailed study. As for CatSper1 and 2[9,10,11], it is likely that human male infertility genes will be found for mutant CatSpers 3, 4, δ, and perhaps β and γ. With 7 subunits of the CATSPER channel identified and a more thorough understanding of CATSPER trafficking in the future, it may be possible to express a functional channel in heterologous systems in order to screen compound libraries for contraceptive agents.

Methods

CATSPER channel complex purification and peptide identification

The CATSPER channel complex was purified from mouse testes by affinity chromatography at 4°C and monitored by CATSPER1 western blotting. 25 frozen mouse testicles (Pel-Freeze Biologicals) were homogenized and microsomes were isolated by step centrifugation in 0.32M sucrose buffer with protease inhibitor cocktail (PIC, no EDTA; Complete, Roche; yield ~850 mg). Microsomal proteins were solubilized in TBS-1% Triton X-100 with PIC and cleared by centrifugation at 100,000g (yield ~400mg). Native CATSPER1 bound to cobalt resin (Talon, Clontech) were eluted from an imidazole gradient. Fractions containing CATSPER1 (~1mg protein) were pooled and bound to immobilized anti-CATSPER1 resin (Protein A Sepharose, Amersham). Bound CATSPER1 complex was washed in high stringency conditions (RIPA+0.2M imidazole) and eluted in 0.1M glycine-0.4% CHAPS, pH 2.5. CATSPER1-copurified proteins were separated by 4–12% gradient SDS gel electrophoresis (Invitrogen) and visualized by Coomassie staining. Proteins purified from identical preparations with immobilized preimmune immunoglobulins were considered nonspecific. Specifically copurified protein bands were excised and in-gel digested with trypsin. Dried peptides were dissolved in matrix, subjected to MALDI-TOF MS and MS/MS analyses using a 4700 Proteomics analyzer and GPS software (Applied Biosystems). A combination of peptide mass fingerprinting and the MS/MS analysis was performed using the Mascot search engine (Matrix Science). Collision-induced dissociation spectra were submitted for protein identification with a precursor precision tolerance of 1Da and MS/MS fragment tolerance of 0.5Da.

Multiple tissue RT-PCR

PCR was performed according to standard protocols using a commercial multiple panel cDNA template (MTC, Clontech). PCR primers amplified *Tmem146* from exons 16 to 19 (forward: TCAACTTCACTGCCAGCATC, reverse: TCCCATTCTTCCACAGTTCC) using mouse *G3PDH* as control.

Molecular cloning

The complete coding sequence of *Tmem146* was assembled by 5′ RACE amplification (Marathon Ready Mouse Testis cDNA, Clontech) using cDNA fragment-specific antisense (GSP2: GATGTTGATGTTGGC and GSP3: GGAGCCTTTGAAACAACAAACGTCACCA) and an AP primer. Two splice variants were detected by RT-PCR with the RACE identified 5′-sequence as forward (RT-5′:CAAGATGCTGGTGTTGATGC) and two reverse primers (Fig. 2b, upper with GSP3 and lower with GSP2). Full-length *Tmem146* cDNAs were obtained by RT-PCR with primers to the RT-5′ and 3′-end (CTATGTCTCTGGATGTTTCTGGGCAACTCG). Sequencing the TOPO-cloned PCR products into pCR4-TA (Invitrogen) confirmed the assembled *Tmem146* cDNAs.

In situ hybridization

10μm thick paraffin sections of 4% paraformaldehyde fixed mouse testes were probed with digoxigenin-labeled antisense RNA probes. Probe 1 corresponds to 1078 bp covering exons 14–22 (forward: GGCAACTCTAAGTACAAACT and reverse: ATGTCTCTGGATGTTTCTGGG) and Probe 2 corresponds to 448 bp of exons 4/6–10 (excluding exon 5; forward: CAAGTCATTGGCGGTATATCAG and reverse: GCACGTGTTCAACAATCTGG). Antisense probe 2 is completely complementary to the *Tmem146-s* and forms an antisense-target RNA duplex for detection of the small transcript. Probe 2 is either partially complementary to *Tmem146-l*, with 13 bp tandem mismatches at its 3′ end, or requires an 118 bp region of bulged nucleotides in *Tmem146-l* mRNA in order to form the 3′ duplex. In either case, hybridization of Probe 2 with *Tmem146-l* is thermodynamically less favorable than the hybridization with *Tmem146-s*[33] and is most likely to report mRNA expression of *Tmem146-s*.

Real-time qRT-PCR analysis for *CatSpers* expression

Real time PCR was carried out with first strand cDNAs from 2μg total testis RNA using the SYBR Green (RT^2 Real-Time SYBR Green/ROX PCR, SABiosciences; Eppendorf Realplex). Quantitative analysis by the ΔΔCt method[34] employed TATA box binding protein (TBP) as amplification controls. Three independent sets of experiments were performed to calculate fold changes ($2^{-\Delta\Delta Ct}$) of *CatSpers* mRNA. The primers used for qRT-PCR were: *CatSper1* (forward1: CTGCCTCTTCCTCTTCTCTG, reverse1: TGTCTATGTAGATGAGGGACCA and forward2: GCAAATGATATTGTCACTGACC, reverse2: CATGAAGTACCATTCACCTCG), *CatSperβ* (forward: CCTTATTGACCAAGAAACAGAC, reverse: TGAAACCCATATTTGACTGCC), *CatSperγ* (forward1: TGAGCAATAGAGGTGTAGAC, reverse1: CAGGATGTAGAAGACAACCAG and forward 2: GATCCGTCAGAGAACTATTTGAG, reverse2: GGAGTCCACCATCAAATACATGG), *CatSperδ* (forward1: GAAGCATACGATCCTATCAACC, reverse1: CCATTCTTCCACAGTTCCAC and forward2: GTCGAGTATCAGGTCTTAGG, reverse2: GTTGCAGTAGCTGTAGTATGG), and *TBP* (forward: GCTGACCCACCAGCAGTTCAGTA, reverse: AAGGAGAACAATTCTGGGTTTG). For specific detection of *Tmem146* splice variants, *Tmem146-l* (forward: GCTGACATTTCTGTGTATCTAGG, reverse:

CTGATATACCTTCCAATTTACGCC), *Tmem146-s* (forward: GCTGACATTTCTGTGTATCTAGG, reverse: CTGATATACCGCCAATGACTTGG).

Antibodies

Anti-CATSPER1, 3, and 4 antibodies were described[5,6]. Peptides corresponding to amino acids 446–459 (α-δ446: DGNSKYKLDIELKQ) and 786–805 (α-δ786: RRVKDQNRGKVRVAQKHPET) of CATSPERδ, 884–899 (TDNFYHADPSKPIPRN) of CATSPERβ, and 53–73 (KFEKVGLHLSKDRFQDHEPID) of CATSPERγ, 21–39 (α-LOC75721: DDHQLSESLSEDYDLPDYD) of hypothetical protein LOC75721 (NP_898936), 74–90 (α-SLC39A6: EGFRKLLQNIGIDKIKR) of zinc transporter ZIP6 precursor (SLC39A6), and 29 – 42 (α-SLC39A7: EGHGDLHKDVEEDF) of zinc transporter SLC39A7 were synthesized and conjugated to KLH carrier protein to produce antiserum (Open Biosystems). The antisera were affinity purified on the immobilized resin of the corresponding peptide (Amino Link plus, Pierce). Anti-V5 and anti-α tubulin antibodies are from Invitrogen and Cell Signaling Technologies, respectively.

Immunocytochemistry

Sperm cells from the *cauda epididymis* attached to glass coverslips were fixed in 4% paraformaldehyde in PBS, permeabilised with 0.2% TrixonX-100 for 5min, washed in PBS and blocked with 10% goat serum for 1h. Samples were stained overnight with primary antibody against CATSPERδ (a-δ446, 10μg/ml) in 10% goat serum, 4°C. After PBS wash, goat-anti-rabbit Alexa568 conjugate (Molecular Probes) served as secondary antibody. Images were acquired by confocal microscopy (Olympus Fluoview 1000).

Tmem146 targeting construct and analysis of ES cell clones

A mouse *Tmem146* gene fragment was isolated from a BAC clone and the targeting construct created by recombineering[20]. Materials for homologous recombination were provided by the NCI-Frederick Institute (http://recombineering.ncifcrf.gov/). The targeting construct was linearized and electroporated into ES cells derived from 129/SvJ1 mice for homologous recombination. G418-resistant colonies were selected and clones carrying mutated *Tmem146* genomic sequences at the proper locus (5F: GAGGTTCAATTTCCAGCAGTC, 5R1: GACGTGCTACTTCCATTTGTC, 3F: TACCCGTGATATTGCTGAAGAG, 3R: GGAGGGAGATAGACAAGACAC) identified. The ES cell clone harboring the targeting construct (clone 97) were transfected with pOG231, a plasmid for transient *Cre* expression, to excise the neomycin cassette and create the conditional *null* allele. Subsequent subclones (clones 97-*Cre*) with the appropriate recombination of *loxP* sites were genotyped (5F: GAGGTTCAATTTCCAGCAGTC, 5R2: GTGATGACCCATAAATGTTGCC).

Generation of *CatSperδ*-deficient mice and genotyping of mutant mice

Three mutant ES cell clones (97-*Cre*) were injected into C57BL/6 blastocysts and transplanted into the uterus of pseudopregnant foster mothers. Chimeric animals were bred with C57BL/6 to obtain heterozygous offspring. Initially, genotype analysis was performed by PCR on isolated genomic DNA (5F and 5R2). F2 heterozygous mice genotyping was

done by Transnetyx Inc. Mice used in the study were the offspring of crosses between F1 and/or F2 generations (50% 129/SvJ and 50% C57BL/6J genetic background). Mice were treated in accordance with guidelines approved by the Children's Hospital Animal Care and Use Committee.

Analysis of *Tmem146* mRNAs from different mouse genotypes

First strand cDNAs were prepared from 1 μg total RNA of *wt*, *het* or *null* testes using oligo(dT) primers and reverse transcriptase using a Superscript III first strand kit (Invitrogen). The forward primer spanning exon 7 and 8 (CTGACAAACTGAGTCACCTG) and the reverse primer corresponding to exon 12 (GACTGCACATTCACTGTACAC) amplified 561 and 410bp from the *wt* and mutant cDNAs, respectively.

Western blotting and immunoprecipitation

Spermatozoa from the *cauda epididymis* were washed and suspended in PBS, counted in a hemocytometer, and lysed directly in 2xLDS sample buffer with 50mM dithiothreitol (DTT). Lysates corresponding to either 5×10^5 or 1×10^6 spermatozoa were analyzed by Western blotting. Testes were solubilized in lysis buffer (T-PER, Pierce) supplemented with a PIC. Solubilized proteins cleared by centrifugation (14,000xg) were immunoprecipitated with anti-CATSPER1, β, δ786, or γ. Proteins were detected with horseradish peroxidase-conjugated anti-rabbit IgG.

Flagellar beat and waveform analysis

Spermatozoa from dissected *cauda* epididymis (swim upward method) were collected in HS media containing (in mM): 135 NaCl, 5 KCl, 2 $CaCl_2$, 1 $MgSO_4$, 20 HEPES, 5 Glucose, 10 lactic acid, 1 Na pyruvate, pH 7.4 (with NaOH). Spermatozoa were plated on 35mm coverslips for 15min (22°C); unattached sperm were removed by gentle pipette wash (time 0) and basal beat frequencies recorded. Activated motility was recorded within the first 10min after adding pre-warmed HTF capacitating medium (in mM): 102 NaCl, 4.7 KCl, 2 $CaCl_2$, 0.2 $MgCl_2$, 0.37 KH_2PO_4, 2.78 glucose, 18.3 lactic acid, 0.33 Na pyruvate, 25 HCO_3- and 4mg/ml BSA). To induce hyperactivation, attached sperm cells were incubated in HTF media for 90min at 37°C (5% CO_2). All subsequent images were recorded at room temperature. The flagellar waveform was analyzed by stop-motion digital imaging collected at 60Hz (XCAP image processing software; EPIX; 2s movies). Beat frequency of each sperm cell was calculated as one-half of the time elapsed for 2 complete flagellar beats. The bending angle, α, of the sperm tail was measured using ImageJ software.

Electrophysiological recording of mouse spermatozoa

Whole-cell recording of *corpus epididymal* spermatozoa from mice 3–5 months of age was performed[1,8]. The standard bath solution, HS, is described above. After break-in, the access resistance was 25–80MΩ. The standard pipette solution was (mM): 115 Cs-Methanesulfonate (Cs-$MeSO_3$), 5 CsCl, 10 Cs_4-BAPTA, 10 HEPES, and 10 MES, pH 7.2 with H-$MeSO_3$. $I_{CatSper}$ was measured as a monovalent current in divalent-free conditions (mM): 150 Na-$MeSO_3$, 2 Na_3HEDTA, 2 EGTA, 20 HEPES; pH 7.4 with NaOH. I_{KSper} was recorded in bath solution containing (mM): 150 K-$MeSO_3$, 10 K-HEPES, and 10 MES (pH

7.4). All experiments were performed at 22–24°C. All currents were recorded using an Axopatch 200B amplifier, acquired with Clampex (pClamp9) (Molecular Devices) and analyzed with Origin software (Originlab). Signals were low pass filtered at 2kHz and sampled at 10kHz. Data are mean ± SEM.

Statistical analysis

Paired two-tailed (Fig. 5c) and unpaired two-tailed (all other) Student's *t*-tests yielded *P* values as listed.

Supplementary Material

Refer to Web version on PubMed Central for supplementary material.

Acknowledgments

We thank the Gene Manipulation Facility of the Children's Hospital Mental Retardation and Developmental Disabilities Research Center (IDDRC, grant no.: NIHP30-HD18655) for ES cell handling and blastocyst injection; M. Sanguinetti for expression in *Xenopus* oocytes, and J. Jun for technical help with antibody work and immunoblotting, A. Riccio for aid with generating the knockout construct, N. Blair for advice on sperm Movie analysis, X. Cai for analysis and discussion of CATSPERδ ortholog sequences, and K. Miki for critical comments on the manuscript. This work was supported by a grant from the National Institutes of Health NINCDS (2 U01 HD045857-06). Mice were treated in accordance with guidelines approved by the Children's Hospital Animal Care and Use Committee.

References

1. Kirichok Y, Navarro B, Clapham DE. Whole-cell patch-clamp measurements of spermatozoa reveal an alkaline-activated Ca^{2+} channel. Nature. 2006; 439:737–740. [PubMed: 16467839]
2. Carlson AE, et al. Identical phenotypes of CatSper1 and CatSper2 null sperm. J Biol Chem. 2005; 280:32238–32244. [PubMed: 16036917]
3. Carlson AE, et al. CatSper1 required for evoked Ca^{2+} entry and control of flagellar function in sperm. Proc Natl Acad Sci USA. 2003; 100:14864–14868. [PubMed: 14657352]
4. Jin J, et al. Catsper3 and Catsper4 are essential for sperm hyperactivated motility and male fertility in the mouse. Biol Reprod. 2007; 77:37–44. [PubMed: 17344468]
5. Qi H, et al. All four CatSper ion channel proteins are required for male fertility and sperm cell hyperactivated motility. Proc Natl Acad Sci USA. 2007; 104:1219–1223. [PubMed: 17227845]
6. Ren D, et al. A sperm ion channel required for sperm motility and male fertility. Nature. 2001; 413:603–609. [PubMed: 11595941]
7. Quill TA, et al. Hyperactivated sperm motility driven by CatSper2 is required for fertilization. Proc Natl Acad Sci U S A. 2003; 100:14869–14874. [PubMed: 14657366]
8. Navarro B, Kirichok Y, Clapham DE. KSper, a pH-sensitive K^+ current that controls sperm membrane potential. Proc Natl Acad Sci U S A. 2007; 104:7688–7692. [PubMed: 17460039]
9. Avidan N, et al. CATSPER2, a human autosomal nonsyndromic male infertility gene. Eur J Hum Genet. 2003; 11:497–502. [PubMed: 12825070]
10. Avenarius MR, et al. Human male infertility caused by mutations in the CATSPER1 channel protein. Am J Hum Genet. 2009; 84:505–510. [PubMed: 19344877]
11. Hildebrand MS, et al. Genetic male infertility and mutation of CATSPER ion channels. Eur J Hum Genet. 2010; 18:1178–1184. [PubMed: 20648059]
12. Liu J, Xia J, Cho KH, Clapham DE, Ren D. CatSperβ, a novel transmembrane protein in the CatSper channel complex. J Biol Chem. 2007; 282:18945–18952. [PubMed: 17478420]
13. Wang H, Liu J, Cho KH, Ren D. A novel, single, transmembrane protein CATSPERγ is associated with CATSPER1 channel protein. Biol Reprod. 2009; 81:539–544. [PubMed: 19516020]

14. Ho K, Wolff CA, Suarez SS. *CatSper-null* mutant spermatozoa are unable to ascend beyond the oviductal reservoir. Reprod Fertil Dev. 2009; 21:345–350. [PubMed: 19210926]
15. Xia J, Ren D. The BSA-induced Ca^{2+} influx during sperm capacitation is CATSPER channel-dependent. Reprod Biol Endocrinol. 2009; 7:119. [PubMed: 19860887]
16. Xia J, Ren D. Egg coat proteins activate calcium entry into mouse sperm via CATSPER channels. Biol Reprod. 2009; 80:1092–1098. [PubMed: 19211808]
17. Quill TA, Ren D, Clapham DE, Garbers DL. A voltage-gated ion channel expressed specifically in spermatozoa. Proc Natl Acad Sci U S A. 2001; 98:12527–12531. [PubMed: 11675491]
18. Divjak M, Glare EM, Walters EH. Improvement of non-radioactive in situ hybridization in human airway tissues: use of PCR-generated templates for synthesis of probes and an antibody sandwich technique for detection of hybridization. J Histochem Cytochem. 2002; 50:541–548. [PubMed: 11897807]
19. Cai X, Clapham DE. Evolutionary genomics reveals lineage-specific gene loss and rapid evolution of a sperm-specific ion channel complex: CatSpers and CatSperbeta. PLoS One. 2008; 3:e3569. [PubMed: 18974790]
20. Liu P, Jenkins NA, Copeland NG. A highly efficient recombineering-based method for generating conditional knockout mutations. Genome Res. 2003; 13:476–484. [PubMed: 12618378]
21. Platts AE, et al. Success and failure in human spermatogenesis as revealed by teratozoospermic RNAs. Hum Mol Genet. 2007; 16:763–773. [PubMed: 17327269]
22. Chen Y, et al. Soluble adenylyl cyclase as an evolutionarily conserved bicarbonate sensor. Science. 2000; 289:625–628. [PubMed: 10915626]
23. Esposito G, et al. Mice deficient for soluble adenylyl cyclase are infertile because of a severe sperm-motility defect. Proc Natl Acad Sci U S A. 2004; 101:2993–2998. [PubMed: 14976244]
24. Martinez-Lopez P, et al. Mouse sperm K^+ currents stimulated by pH and cAMP possibly coded by Slo3 channels. Biochem Biophys Res Commun. 2009; 381:204–209. [PubMed: 19338774]
25. Schreiber M, et al. Slo3, a novel pH-sensitive K^+ channel from mammalian spermatocytes. J Biol Chem. 1998; 273:3509–3516. [PubMed: 9452476]
26. Santi CM, et al. The SLO3 sperm-specific potassium channel plays a vital role in male fertility. FEBS Lett. 2010; 584:1041–1046. [PubMed: 20138882]
27. Li HG, Ding XF, Liao AH, Kong XB, Xiong CL. Expression of CatSper family transcripts in the mouse testis during post-natal development and human ejaculated spermatozoa: relationship to sperm motility. Mol Hum Reprod. 2007; 13:299–306. [PubMed: 17347248]
28. Nikpoor P, Mowla SJ, Movahedin M, Ziaee SA, Tiraihi T. CatSper gene expression in postnatal development of mouse testis and in subfertile men with deficient sperm motility. Hum Reprod. 2004; 19:124–128. [PubMed: 14688170]
29. Catterall WA. Ion channel voltage sensors: structure, function, and pathophysiology. Neuron. 2010; 67:915–928. [PubMed: 20869590]
30. Dolphin AC. Calcium channel diversity: multiple roles of calcium channel subunits. Curr Opin Neurobiol. 2009; 19:237–244. [PubMed: 19559597]
31. Pazour GJ, Bloodgood RA. Targeting proteins to the ciliary membrane. Curr Top Dev Biol. 2008; 85:115–149. [PubMed: 19147004]
32. Pongs O, Schwarz JR. Ancillary subunits associated with voltage-dependent K^+ channels. Physiol Rev. 2009; 90:755–796. [PubMed: 20393197]
33. McFadden GI. *In situ* hybridization. Methods Cell Biol. 1995; 49:165–183. [PubMed: 8531753]
34. Schmittgen TD, Livak KJ. Analyzing real-time PCR data by the comparative C(T) method. Nat Protoc. 2008; 3:1101–1108. [PubMed: 18546601]

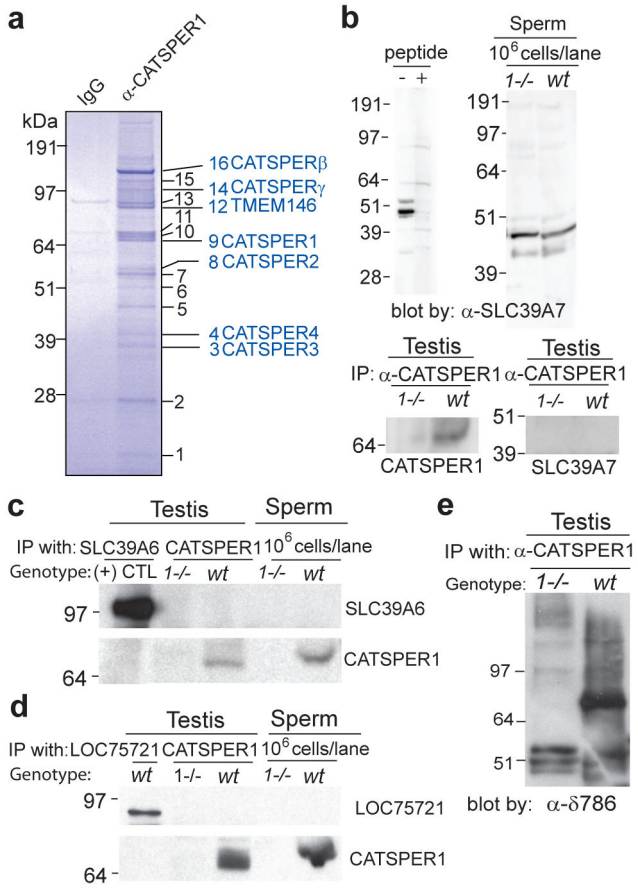

Figure 1. Identification of CATSPERδ encoded by *Tmem146* as an auxiliary subunit of native CATSPER channels

(**a**) Purified CATSPER1 complex (α-CATSPER1) separated by SDS-PAGE and stained with Coomassie blue. Rabbit IgG column eluate serves as control (IgG). Numbered protein bands in the purified CATSPER1 complex were subjected to mass spectrometry identification. Confirmed CATSPER1 interactors are listed (blue). The CATSPER channel in the testis is comprised of a macromolecular complex of all four α subunits (CATSPERS1-4), two previously identified auxiliary subunits (CATSPERβ and γ) and a novel auxiliary subunit, TMEM146 (CATSPERδ). (**b** and **c**) Two transmembrane proteins that did not express specifically in testes, SLC39A7 (band 5) and SLC39A6 (band 12), were tested for potential interaction with CATSPER1. Anti-SLC39A7 antibody recognized protein in spermatozoa, but its expression was not CATSPER1-dependent. Interaction with CATSPER1 was not found in testis (b). SLC39A6 antibody detected recombinant protein expressed in HEK293T cells ((+) CTL), but no protein was detected in sperm cells or in the CATSPER1 complex (c). (**d** and **e**) Two novel testis-specific proteins from band 12 were tested for potential interaction with CATSPER1. LOC75721 was expressed in testis but not in the CATSPER1 immune complex or sperm cells (d). Another protein identified from band12, TMEM146/CATSPERδ co-immunoprecipitates with CATSPER1 (e).

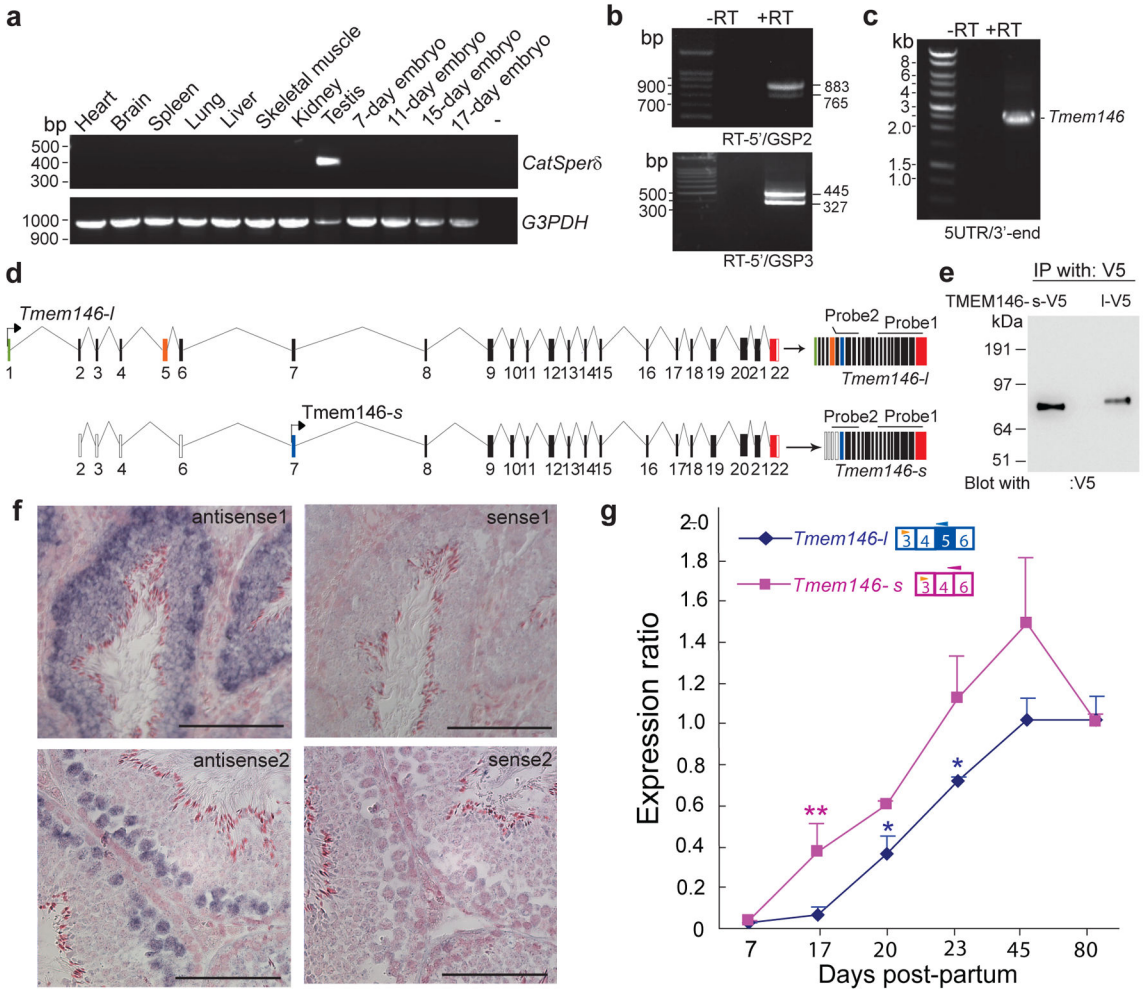

Figure 2. Molecular cloning of two alternative splice variants of *CatSperδ*

(**a**) Tissue distribution of *CatSperδ* mRNA by reverse-transcription PCR. *CatSperδ* (*upper*) and *Glyceraldehyde-3-Phosphate Dehydrogenase* (control; *lower*) from 12 mouse cDNAs; negative control (*lane "−"*). *CatSperδ* was detected only in testis. (**b** and **c**) Molecular cloning of *CatSperδ* cDNAs. Two bands differing by 118 bp were amplified by mouse testis first-strand cDNAs by PCR with primers corresponding to the most upstream 5′ sequence identified by 5′-RACE and 2 different gene-specific primers (GSP) nested at the 5′-UTR of *Tmem146-s*. RT, reverse transcriptase (b). Whole open reading frames (ORFs) of *Tmem146* were amplified from testis cDNA (c). (**d**) Schematic diagram of *CatSperδ* splice variants. Two alternatively spliced mRNA variants are transcribed from the *Tmem146* gene. *Tmem146-s* has a start site in exon 7 (blue). *Tmem146-l* contains a new start site in exon 1 (green) due to a change in the ORF by the additional 118 bp exon 5 (orange). The locations of probes for *in situ* hybridization are illustrated above the transcripts. Probe 1 is complementary to both *Tmem146-s* and *–l*. Probe 2 was amplified from *Tmem146-s* cDNA and corresponds to the splicing region (spanning exon 4 and 6). (**e**) Heterologous expression of CATSPERδ isoforms. V5-tagged *Tmem146-s* or *Tmem146-l*, cDNAs were transfected into HEK293T cells. After immunoprecipitation with anti-V5, immune complexes were probed with anti-V5. **(f)** Spatial localization of *Tmem146* splice variants. Representative fields of *in situ* hybridization in mouse testis using antisense 1 (*upper left*) and antisense 2 (*lower left*). Sense probes served as background controls (*right panels*). Scale bar, 100 μm. (**g**) Temporal *Tmem146-s* and *Tmem146-l* mRNA levels (real time RT-PCR) during testis postnatal development. mRNAs are normalized to TATA binding protein (TBP) at each time point and expressed as ratios relative to adult (80-day) mouse testis (± SEM compared to each prior time point *$P < 0.05$,

**$P < 0.005$). *Tmem146-s* mRNA was detected at 17 days (unpaired two-tailed *t*-test, $P = 0.0017$) while *Tmem146-l* appeared at 20 days ($P = 0.047$ at 20 days, $P = 0.042$ at 23 days), consistent with the *in situ* hybridization experiments. Results are from 3 independent experiments.

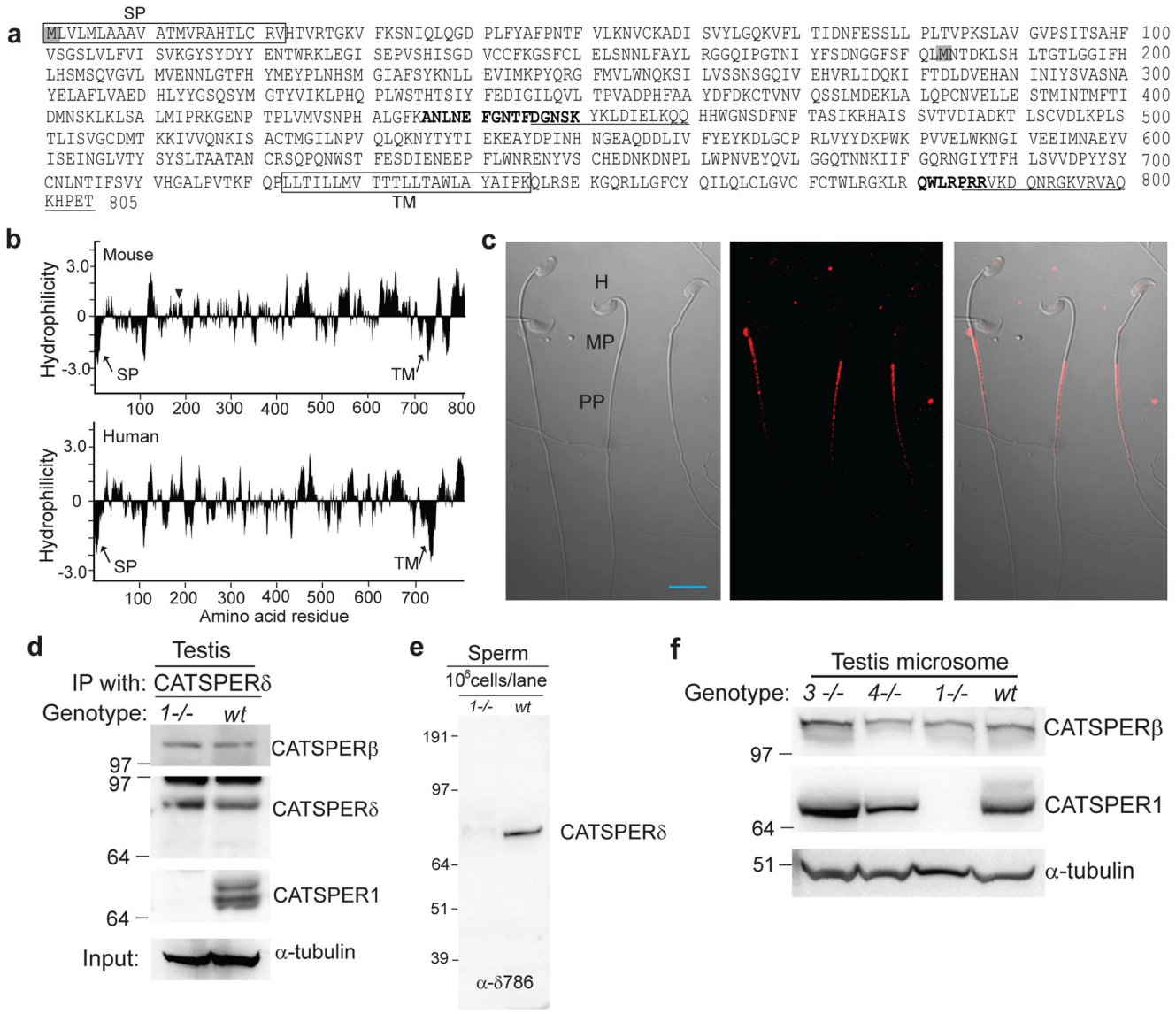

Figure 3. Characterization of the CATSPERδ protein

(**a**) Predicted mouse CATSPERδ protein sequences. Predicted signal peptide (SP) and transmembrane (TM) domain are boxed. The two peptides identified by mass spectrometry are in **bold** (amino acids 436–450 and 781–787). Two peptide epitopes used to generate antibodies are underlined (amino acids 446–470 and 786–805). The first methionines of two potential TMEM146 isoforms are shadowed in grey. (**b**) Hydrophilicity plots (window size, 11) of mouse (*upper*) and human (*lower*) CATSPERδ. The predicted signal peptide and the single transmembrane domain (TM) are marked by arrows. The alternative start site of *Tmem146-s* is marked by the arrowhead. (**c**) Immunostaining of mouse sperm by α-CATSPERδ (α-δ446). *Left*, phase contrast image. The head (H), midpiece (MP), and principal piece (PP) of the sperm are indicated. *Middle*, immunofluorescence; *right*, merged signal. Scale bar, 10 μm. (**d**) Interaction of CATSPER1, CATSPERβ, and CATSPERδ in *wt* testes (*wt*). CATSPERδ is associated with CATSPERβ regardless of CATSPER1 expression (*1−/−*). α-tubulin; input control. (**e**) Absence of CATSPERδ protein in *CatSper1-null* spermatozoa. (**f**) Expression of CATSPER1 and CATSPERβ in the testis of homozygous null *CatSper1 (1−/−)*, *CatSper*3 *(3−/−)*, and *CatSper4 (4−/−)* and wild type (wt) mice.

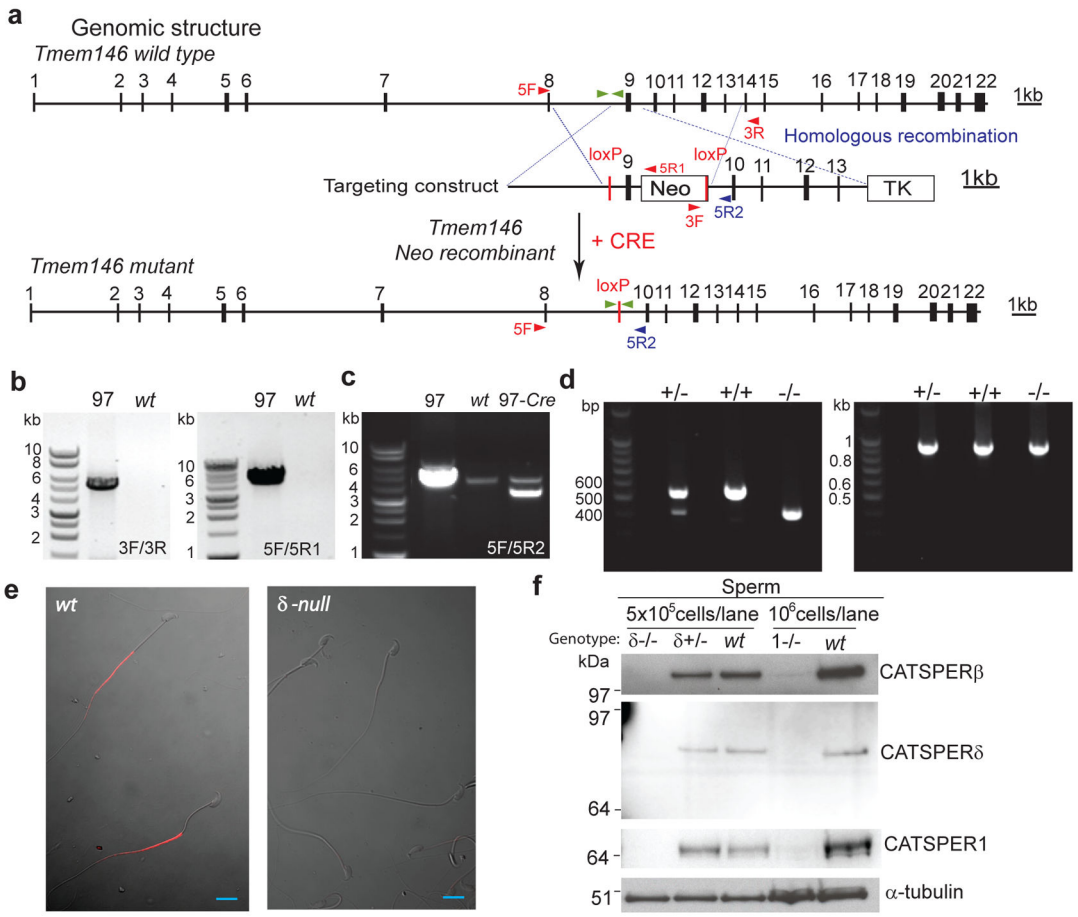

Figure 4. Targeted disruption of *Tmem146* gene inactivates *CatSperδ*

(a) Whole genomic structure of mouse *Tmem146* gene, targeting construct, and predicted mutant allele generated by homologous recombination and *Cre* excision; *Filled boxes*, exons; *thin lines*, introns. Neomycin (Neo) and thymidine kinase (TK) selection cassettes are shown. The locations of primers used for genotyping are shown with arrowheads. Primers located outside targeting region, 5F and 3R; inside targeting region, 5R2; within *Neo*, 5R1 and 3F. (**b** and **c**) PCR genotyping of genomic DNA. *Tmem146 Neo* mutant ES clone (97) is identified by the presence of PCR products at both the 3′- (3F/3R) and 5′- (5F/5R2) of the expected locus (b). Excision of genomic sequence flanked by two *loxP* sites by PCR with 5F/5R2 (c). **(d)** RT-PCR of *CatSperδ* with testis mRNA from *CatSperδ–null* mice showing the expected products. Combination of two primers with one spanning exon 7/8 and the other in exon 12 demonstrates absence of exon 9 in the *CatSperδ* transcript (*left*). RT-PCR of *GAPDH* is the control (*right*), *CatSperδ null–*(−/−), *CatSperδ–heterozygotes* (+/−) and wildtype (+/+). **(e)** Immunostaining of mouse epididymal sperm with anti-CATSPERδ antibody (α-δ446). CATSPERδ specifically labels only the principal piece of the tail of *wt* spermatozoa (*left*) and is not observed in the *CatSperδ-null* sperm cells (*right*). Scale bar, 10 μm. **(f)** Absence of CATSPER1, β and δ proteins in spermatozoa of *CatSperδ* homozygous null mice.

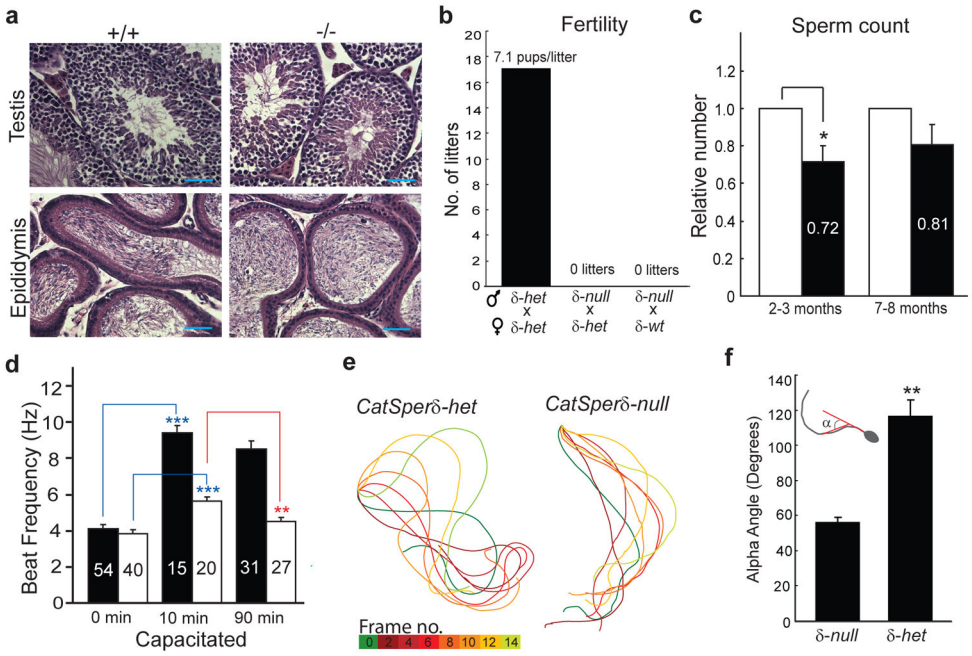

Figure 5. *CatSperδ-null* male mice are infertile and their sperm fail to hyperactivate

(a) Hematoxylin and eosin staining of the testes (*top*) and epididymis (*bottom*) of *wt* (*left*) and *CatSperδ-null* (*right*) mice. Testis morphology is normal. Scale bar, 50 μm. **(b)** *CatSperδ-null* males are infertile. (**c**) Epididymal sperm count (mean ± SEM) from littermates at ages of 2–3 or 7–8 months of age (6 pairs each). *Het* (open)-versus *null* (filled): *P < 0.05, paired two-tailed *t*-test. **(d)** Flagellar beat frequency of *CatSperδ-het* (*open*) and *null* sperm (*filled*). Basal beat frequency immediately after isolation (time 0), beat frequencies of activated (10 min) and hyperactivated (90 min) sperm cells incubated in capacitating media; n = 15–54 tethered sperm cells in 4 independent experiments (unpaired two-tailed *t*-test, ***$P < 0.001$, **$P < 0.005$). **(e)** Aligned flagellar waveform traces. Sperm cells were examined 90 min after incubation in capacitating conditions to induce hyperactivation. Representative traces of single spermatozoa of *CatSperδ-het* and *CatSperδ-null* are shown. *CatSperδ-het* full beat cycle lasted ~230 ms, during which *CatSperδ-null* sperm completed two beat cycles. **(f)** Measurement of bending angle. Capacitated *het* spermatozoa exhibit larger ranges of motion than *CatSperδ-null* spermatozoa as indicated by the maximum bending angle (inset, α; unpaired two-tailed *t*-test, **$P < 0.005$). n=6.

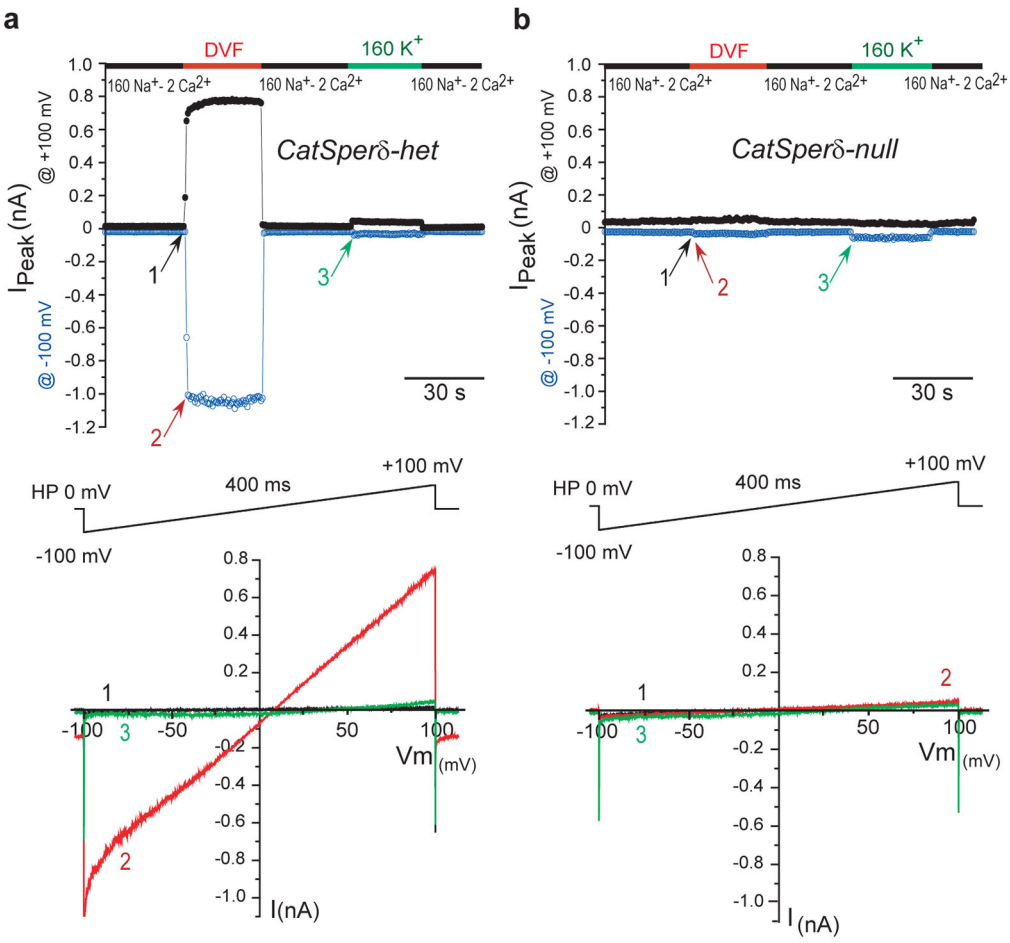

Figure 6. *CatSperδ-null* mice lack CatSper current

(a) *CatSperδ-het* and **(b)** CatSper*δ-null* $I_{CatSper}$. The upper traces show representative time courses of $I_{CatSper}$ measured in control solutions (1), nominally divalent-free (DVF) solutions (2), and high-K^+ solutions (3) at −100 mV (**open cicrles**) and + 100 mV (closed circles). Bottom panels show the current-voltage relations of monovalent $I_{CatSper}$ in response to voltage ramps at the time points indicated. $I_{CatSper}$ is absent in *CatSperδ-null* sperm cells. A small inward I_{KSper} was seen in both phenotypes when the bath solution was switched to 160 mM K-$MeSO_3$. *CatSperδ-het* currents are indistinguishable from previously published *wt* currents[1].

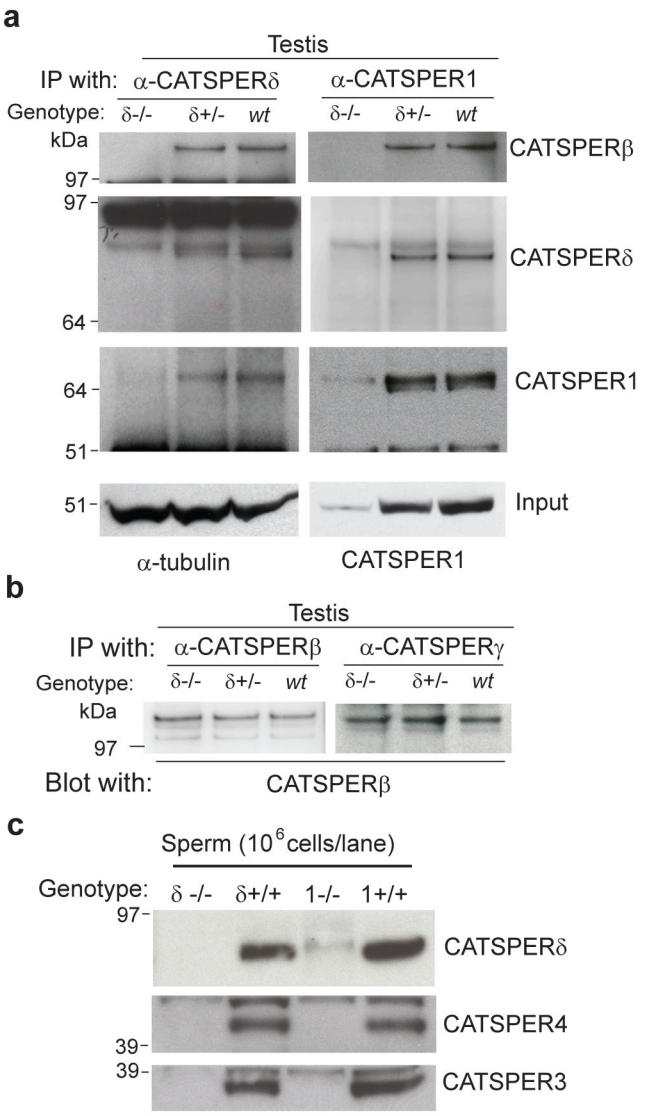

Figure 7. Inactivation of *CatSperδ* decreases the stability of CATSPER1 during spermatogenesis

(a) Reduction of CATSPER1 protein by *CatSperδ* deletion. Proteins solubilized from testis are immunoprecipitated with specific anti-CATSPERδ antibodies (α-δ786, IP, *left*) or anti-CATSPER1 (IP, *right*). CATSPERδ was pulled down from *CatSperδ-het* (*δ*+/−) and *wt* (+/+) testes but not from homozygous mutant testes (*δ*−/−) (IP, *left, middle*). CATSPERβ and CATSPER1 proteins are found in the same protein complex from *CatSperδ-het* and *wt* testes (IP, *left, top, and bottom*). Reciprocally, anti-CATSPER1 antibodies also co-immunoprecipitated CATSPERβ and CATSPERδ (IP, *right, top and middle*) from *CatSperδ-het* and *wt* testes. The amount of CATSPER1 was greatly reduced in the *CatSperδ* homozygous mutants (input, *right*) while input control (α tubulin) was unchanged (input, *left*). A small amount of CATSPER1 was recovered by anti-CATSPER1 immunoprecipitation from homozygous mutant testes (IP, *right, bottom left lane*). **(b)** In *CatSperδ* homozygous null mice, CATSPERβ was associated with CATSPERγ. **(c)** Absence of expression of CATSPER3 and CATSPER4 subunits in the sperm cells of *CatSperδ* homozygous null mice.

Table 1

Proteomic analysis of proteins copurified with CATSPER1.

Band number	*Protein name*	*Accession No.*	*No. of peptides*	Coverage (%)
Testis specific				
9	**CATSPER1**	**21314844**	**8**	**19.7**
8	**CATSPER2**	**124001554**	**4**	**7.9**
3	**CATSPER3**	**30350218**	**6**	**17.6**
***4**	**CATSPER4**	**29244466**	**7**	**18.5**
16	**CATSPERβ**	**257900479**	**34**	**39.3**
14	**CATSPERγ**	**157951745**	**7**	**8.3**
12	**TMEM146**	**261245039**	**2**	**2.7**
12	*Unnamed protein product (hypothetical protein LOC75721)*	*34147101*	*2*	*3.1*
11	HSPA2 (HSP70-2)	123621	15	32.9
Not testis-specific				
*13	PARASPECKLE	225543409	8	14.1
12	*SLC39A6*	*26324938*	*4*	*7.1*
*11	GRP78	1304157	17	34.4
8	Non-POU-domain-containing, octamer binding protein	12963531	13	12.6
7	Cleavage and polyadenylation specificity factor subunit 7	24416453	14	21.6
*6	Tubulin β-2c	22165384	4	10.4
**5*	*SLC39A7*	*6680147*	*3*	*15.9*
*5	Elongation factor Tu	556301	4	8.4
***2**	Cleavage and polyadenylation specificity factor subunit 5	13386106	15	90.3

* Proteins identified from only one of two purifications.

Proteins verified to be in the CATSPER1 complex are in bold. Proteins tested but not found to be in the CATSPER1 complex are listed in italics. All other proteins were not further characterized.